

Topology optimization of the photovoltaic panel connector in high-rise buildings

Xilin Lu^{1a}, Jiaqi Xu^{1b}, Hongmei Zhang^{*1} and Peng Wei²

¹State Key Laboratory of Disaster Reduction in Civil Engineering, Tongji University, 1239 Siping Rd, Yangpu, Shanghai, China

²State Key Laboratory of Subtropical Building Science, School of Civil Engineering and Transportation, South China University of Technology, 381 Wushan Rd, Tianhe, Guangzhou, Guangdong, China

(Received June 20, 2016, Revised February 7, 2017, Accepted March 9, 2017)

Abstract. Photovoltaic (PV) panels are used in high-rise buildings to convert solar energy to electricity. Due to the considerable energy consumption of high-rise buildings, applying PV technology is of great significance to energy saving. In the application of PV panels, one of the most important construction issues is the connection of the PV panel with the main structures. One major difficulty of the connection design is that the PV panel connection consists of two separate components with coupling and indeterminate dimension. In this paper, the gap element is employed in these two separated but coupled components, i.e., hook and catch. Topology optimization is applied to optimize and design the cross-section of the PV panel connection. Pareto optimization is conducted to operate the optimization subject to multiple load scenarios. The initial design for the topology optimization is determined by the common design specified by the Technical Code for Glass Curtain Wall Engineering (JGJ 102-2003). Gravity and wind load scenarios are considered for the optimization and numerical analysis. Post analysis is conducted for the optimal design obtained by the topology optimization due to the manufactory requirements. Generally, compared with the conventional design, the optimized connector reduces material use with improved structural characteristics.

Keywords: photovoltaic panel connector; topology optimization; SIMP; high-rise building; numerical analysis

1. Introduction

High-rise buildings in metropolis consume enormous amount of electrical power. The contradiction of increasing energy demand and supply shortage becomes acute. Photovoltaic (PV) panel is efficient in converting the clean, non-polluting and renewable solar energy to electricity. Since BIPV (Building Integrated with Photovoltaic) firstly integrated in Hong Kong area in 1990s (Yang and Fung 2003), the PV panel experiences continuous and rapid development. In 1994, the US solar energy technology program (SETP) implemented the 'Million Solar Roofs Initiative' (Strahs and Tombari 2006). In 1999, Germany government conducted the 'German 100,000 Roofs Measurement and Analysis Program' (Erge *et al.* 2001). In 2012, the Chinese 12th five-year plan for renewable energy development approved the policy of free connection for PV panels (Zhang and He 2013). Experts estimate that the PV power generation will produce 10% of the total electricity supply by 2030, and by the end of the 21st century, the proportion will be 60% (Lund and Mathiesen 2009). Massive PV panels are applied in high-rise buildings for the clean and economical electric energy.

Because the connectors are used to transfer loads from the PV panel to the main structure, the connection is

an important element to ensure safety of the PV panel application. However, given the rapidly increasing application of PV panels, the uniform code for PV panel connection design is not developed concurrently. In China, the construction design of the PV system is referred to the Technical Code for Glass Curtain Wall Engineering (JGJ 102-2003). The commonly employed curtain wall connection includes point-support and frame-support connectors. The point-support hook connection provides high light permeability, construction flexibility and architectural aesthetics, hence is employed as a possible connection form for the PV panel installation.

The point-support hook connection usually attaches the four corners of the PV panel with the main structure (as shown in Fig. 1) and serves as the stress concentration position. Mainly, the PV panel is attached to the main structure with several hooks on upper and lower frame beam, some weak connections may be used to limit the deformation of the PV panel at the frame column. Without reliable connection design, the PV panel, as large-scale curtain wall structure, exists huge potential security risk in the massive installation of high-rise buildings. However, the commonly applied point-supported hook connector adjusts the glass curtain wall connector for the specific appearance of the PV panel without numerical calculation or optimization. The common design cannot ensure structural safety and usually cause material waste (Zhang *et al.* 2014). Hence the optimization and numerical analysis of the PV panel connection applied in high-rise buildings is a necessity.

This study analyzes the four-point supported hook connector of the PV panel and optimizes the cross-section

*Corresponding author, Associate Professor
E-mail: zhanghongmei@tongji.edu.cn

^aProfessor

^bPh.D. Student

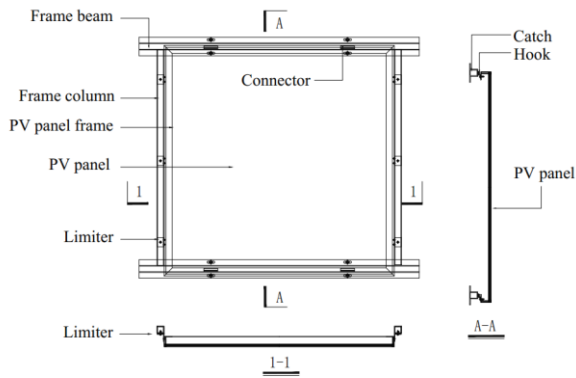


Fig. 1 Schematic diagram of the potential connector

of the connector. The optimized connector is made of stainless steel. The optimized design is based on the structural topology optimization results. The optimized connector consists of two components, hook and catch. In the exemplified project, the hook is connected with the PV panel via a bolt, and the catch is fixed with the main structure by welding. Neither of the dimensions of the two parts can be determined separately, which are, therefore, connected by gap elements and optimized as a whole. The design domain is determined based on the commonly employed potential connectors. The cross-section of the connector is optimized to reduce material use and improve displacement and stress responses. The displacement and stress responses of the conventional and optimized connections are analyzed by finite element analysis (FEA).

2. Method description of topology optimization

To ensure the safety of the PV panel connection for high-rise buildings, this study conducts topology optimization and numerical analysis for the connectors. Topology optimization is one of the most useful and widely applied branch of structural optimization. Haftka and Gürdal (2012) defined the concept of structural optimization as achieving the best outcome of a given operation while satisfying certain restrictions. Structural optimization has undergone rapid development during the last decades, simultaneously in research study and industrial application (Kutyłowski and Rasiak 2014, Lee *et al.* 2012, Lee and Park 2011).

In research, beginning with Michell (1904) showing the economic limit of the material distribution (i.e., the minimum volume in referring paper) of frame structures, structural optimization has become an active research topic and influential instrument to ideate the design concept. Schmit and Farshi (1974) combined mathematical programming methods with structural optimization, making the optimization procedure applicable for practical engineering. Following Schmit, research attention primarily focuses on the minimum weight and maximum stiffness problem with stress or displacement constraints (Kaveh *et al.* 2013). Along with the development of optimization theory, many efficient algorithms have been proposed. For

instance, method based on the concept of duality in convex programming (Fleury 1989), structural synthesis by approximation (Thomas *et al.* 1992), interior-point method (Wright 2004), evolutionary structural optimization (Huang and Xie 2010), etc.

For practical application, topology optimization procedure can be conducted by both large-scale general finite element analysis (FEA) software and public written computer codes. Among the massive commercial FEA software, OptiStruct, developed by Altair Inc., is a front runner in topology optimization. OptiStruct solves the general formulation of the multiple-constraint single-objective topology optimization problem (Zhou *et al.* 2004). The analysis and optimization capability allows OptiStruct to develop preliminary design concepts and improve existing designs as well. Optimality criteria algorithm is applied for the optimization in OptiStruct (Altair Engineering Inc. 2013).

To obtain the optimized PV panel connector design, this study conducts topology optimization and FEA by the OptiStruct software. Because the hook and catch of the connector are separated and coupled in dimension, none of the dimensions can be ensured separately. This study employs gap elements to combine the two components as a whole structure. Contact analysis with contact elements is also provided by the OptiStruct software, which models the contact of a series of nodes with a face. In this study, the contact of the two 2D components is an edge-to-edge problem, which is the limitation of the contact elements. On the other hand, the gap elements can provide rational numerical analysis results for the edge-to-edge contact problem.

Due to the multiple load scenarios considered in this study, the optimization of the connector is a multi-objective problem. Pareto optimization is conducted to convert the multi-objective problem into a single-objective optimization problem. To simplify the manufactory and construction procedure, the design domain of the optimization is the cross-section shape of the connector.

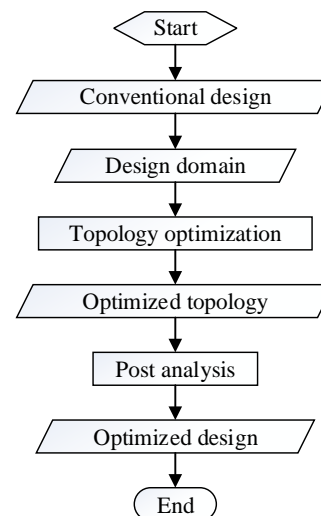


Fig. 2 Flowchart of the optimization procedure
The flowchart of the optimization procedure is shown in

Fig. 2. The optimization procedure consists of two major steps: (i) topology optimization and (ii) post analysis. The optimized design is obtained by the proposed optimization procedure. The conventional design input into the procedure is a commonly applied connector for glass curtain walls. The dimension of the design domain is obtained by enlarging the conventional design to a more general shape to explore more design possibilities. Topology optimization is utilized to optimize the design domain, and the optimized topology of the connector is obtained. By employing the post analysis, the small branches and semi-density elements observed in the optimized topology are removed from the optimized design and an applicable connector design is obtained.

3. Stress and displacement responses of the conventional design

The PV panel connection is commonly designed by adjusting the glass curtain wall connector for the PV panel shape. Because numerical analysis or optimization is not conducted, the commonly applied PV panel connection cannot guarantee structural safety and usually cause material waste. The commonly applied conventional connector design is optimized in this study. This section calculates the displacement and stress responses of the conventional connector design.

3.1 PV module

TSM-PC05A amorphous silicon based solar PV panel (Zhang *et al.* 2014) is taken as the optimization example in this study. Schematic diagram of this PV panel is shown in Fig. 3. The PV module consists of the PV panel and the panel frame. The PV panel frame is the protection and connection part of PV panel, and is made of aluminum alloy. The connector and the main structure are made of stainless steel. The Young's modulus of the applied stainless steel is $E=206$ GPa, and the Poisson's ratio is $\nu=0.3$, as provided by the *Technical Code for Glass Curtain Wall Engineering (JGJ 102-2003)*.

3.2 Conventional design

Fig. 4 illustrates the commonly applied two-part point-support hook connector applied for the PV panel in high-rise buildings. The connectors of PV panels are usually designed based on the connection of stone curtain walls for their similarities as exterior wall curtain structures. The hook connector as shown in Fig. 4 is widely employed in the construction of dry hanging stone curtain walls for the reason that the hanging connection can protect the curtain walls from deformation of the main structure. Furthermore this kind of hook connection are easy to be installed and replace. It is important especially for high-rise buildings (Zeng 2016).

The connector consists of two components: (i) the catch (Fig. 4(a)) and (ii) the hook (Fig. 4(b)). The catch is an 'L' shape protrusion welded with the main structure. The hook

is connected with the PV panel via a bolt and hung on the catch to connect the PV panel with the main structure. Fig. 4(c) is the schematic diagram of the connection. The length of the conventional connector design is 55 mm which is decided by the allowable stress.

The non-flat end part of the conventional hook design is to ensure secure connection. Because the gap between the catch and the main structure is 3 mm and the average width of the left part hook is 2 mm, the non-flat hump is designed to be 3 mm to deadlock the connection and prevent the hook from slipping.

3.3 Numerical analysis

This study focuses on the PV panels on the facade of high-rise buildings. Because high-rise buildings with PV panels are more common in metropolises, Shanghai is taken as the example to determine the load scenario and site condition. The loads and boundary conditions are determined according to the *Load Code for the Design of Building Structures (GB50009-2001)* (referred as 'Load code' below) published by the *Ministry of Construction of People's Republic of China*. In this section, the node displacement and von-Mises stress of the conventional design connector are calculated subjected to self-weight and wind loads transferred from the panel.

3.3.1 Loading scenario

For the connector installed on the facade of high-rise buildings, the major loads are the gravity and the wind load transferred from the PV panel. The four corners of the PV panel are connected with the main structure by four point-support connectors, two at the top and two at the bottom, as shown in Fig. 1. In practical application, the load capacity of the four connectors may be different due to the manufacturing error. To simplify the scenario in this study, the loads are assumed to transfer equally via the four connectors from the panel to the main structure, i.e., each connector undertakes a quarter of the total loads on the panel. For conservative designs, an amplification factor could be multiplied to the design loads, which is not discussed in this paper.

Gravity load

The self-weight of the exemplified PV panel is $m = 30$ kg. The gravity load distributed to each connector is $G = mg/4 = 73.5$ N.

Wind load

In Chinese Load code, site condition is divided into four types (A-, B-, C- and D-type) according to specific geomorphology. 'A-type' site refers to flat landscape, e.g., the sea surface, offshore and desert. 'D-type' site refers to metropolises with massive high-rise structures. In this study, the high-rise building with PV panels is assumed to be located in a C-type site (Shanghai area), i.e., urban area with massive mid- and high-rise buildings. Design wind pressure (w_k) is the measurement of the wind load on the facade of buildings. Four parameters are employed to calculate the wind load pressure:

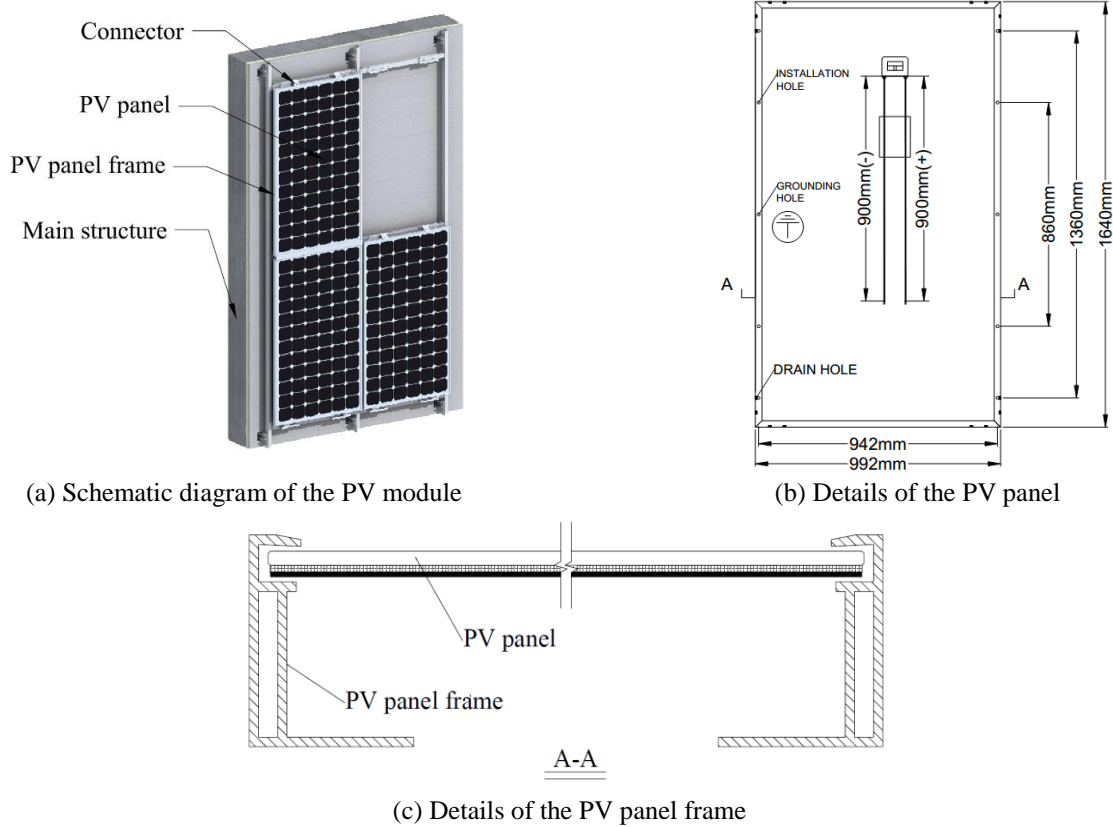


Fig. 3 The schematic diagram of PV panel

- Gust factor β_{gz} . The gust factor modifies the dynamic effect of the wind pressure.
- Shape coefficient μ_{sl} . The shape coefficient modifies the influence of the facade shape.
- Height coefficient μ_z . The height coefficient modifies the wind pressure at different height.
- Basic wind pressure ω_0 . The basic wind pressure is the average wind pressure occurs in 50-year frequency. The statistic wind pressure data of major cities and area in China is estimated in the Load code.

Both the windward (left wind) and leeward (right wind) scenarios should be considered. The design wind load pressure is perpendicular to the facade, and the magnitude is

$$\omega_k = \beta_{gz} \mu_{sl} \mu_z \omega_0 \quad (1)$$

where ω_k is the design wind pressure (kN/m^2). The height of the exemplified building is assumed to be 100 m. At 100 m height in C-type site, the gust factor $\beta_{gz}=1.6$, and the height coefficient $\mu_z=1.7$. For the building with normal facade shape, the shape coefficient $\mu_{sl}=1.5$. In Shanghai area, the basic wind pressure $\omega_0=0.40 \text{ kN/m}^2$. Substituting the values and calculating by Eq. (1), $\omega_k=1.632 \text{ kN/m}^2$. The facade area of the exemplified PV panel is $1 \text{ m} \times 1.65 \text{ m}$. Therefore, the design static wind load is $Q_w=1.632 \text{ kN/m}^2 \times 1 \text{ m} \times 1.65 \text{ m}/4=673.2 \text{ N}$.

Load combination

The combination of the gravity (G) and wind load (Q_w) magnifies both loads by combination coefficients.

Considering wind as the critical load, the combination coefficients of the gravity and wind load (Γ_G and Γ_Q) are 1.2 and 1.4, respectively.

In summary, for each connector, the design gravity load is 88.2 N and the design wind load is $\pm 942.48 \text{ N}$ (the sign function is for distinguishing the leeward/windward direction). The loads are assumed to be evenly distributed along the hook surface connected with the PV panel, as shown in Fig. 5.

3.3.2 Boundary condition

The boundary condition of the conventional design is illustrated in Fig. 5. The PV panel is connected with the hook by a bolt. The material below the bolting point is omitted in the analysis and optimization, because this material is not on the load transferring path. Subject to the windward wind load, the PV panel is assumed to transfer the wind load evenly to the right edge of the hook by the bolt (as shown in Fig. 5 (a)-(b)). Subject to the leeward wind load, the loading point on the hook is at the left edge of the bolting position (as shown in Fig. 5 (c)-(d)). The gravity and wind load are assumed to be evenly distributed along the connecting surface with the bolt. Fig. 5 (b) and Fig. 5 (d) are the schematic diagram of the finite element meshes, boundary conditions and loading positions.

The catch is welded with the main structure, hence in both wind loading direction, the boundary of the inner side of the catch is fixed. The L-shape catch is connected with the hook by gap elements. The 'pseudo gap element' is

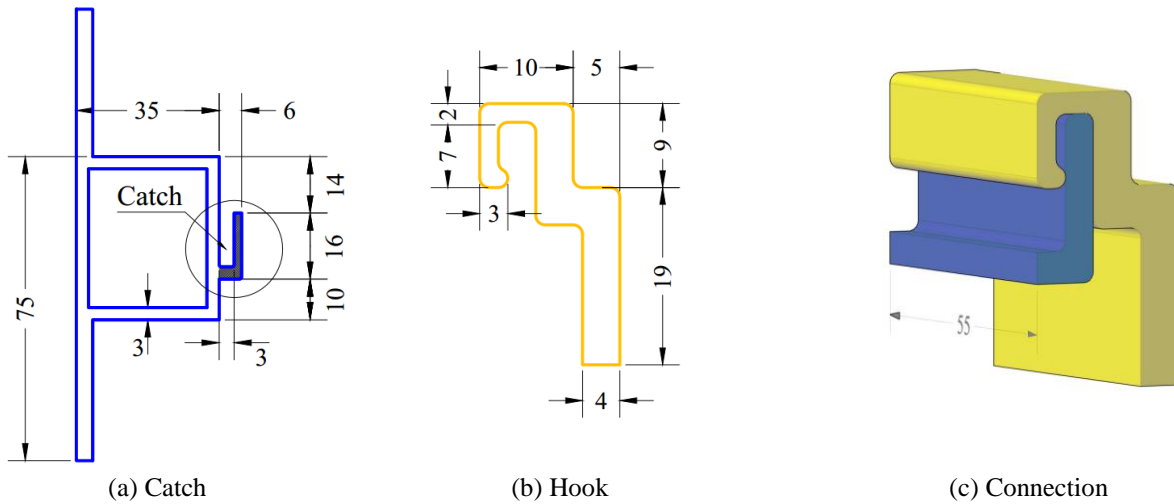


Fig. 4 Conventional connection design (unit: mm)

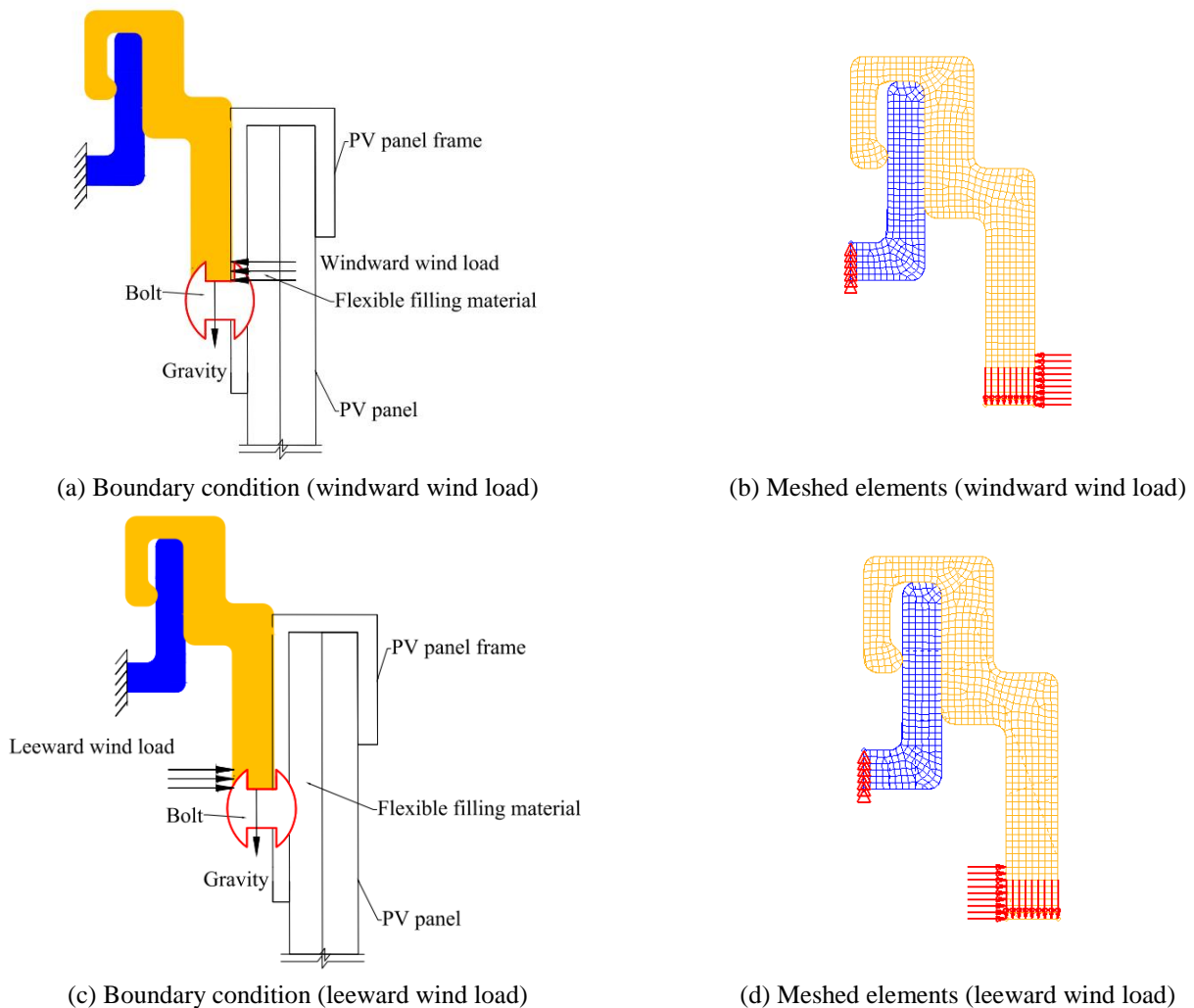


Fig. 5 Conventional design

applied to simulate the contact problem. The gap element is a 1D element created in the space between the hook and catch where contacting may occur. At the non-contact domain, the gap element has no influence on the elements.

When contact occurs, i.e., the relative displacement of the connected two nodes is less than the initial gap opening, the normal stiffness is equal to the component material to prevent contact elements from intrusion. In this analysis, the

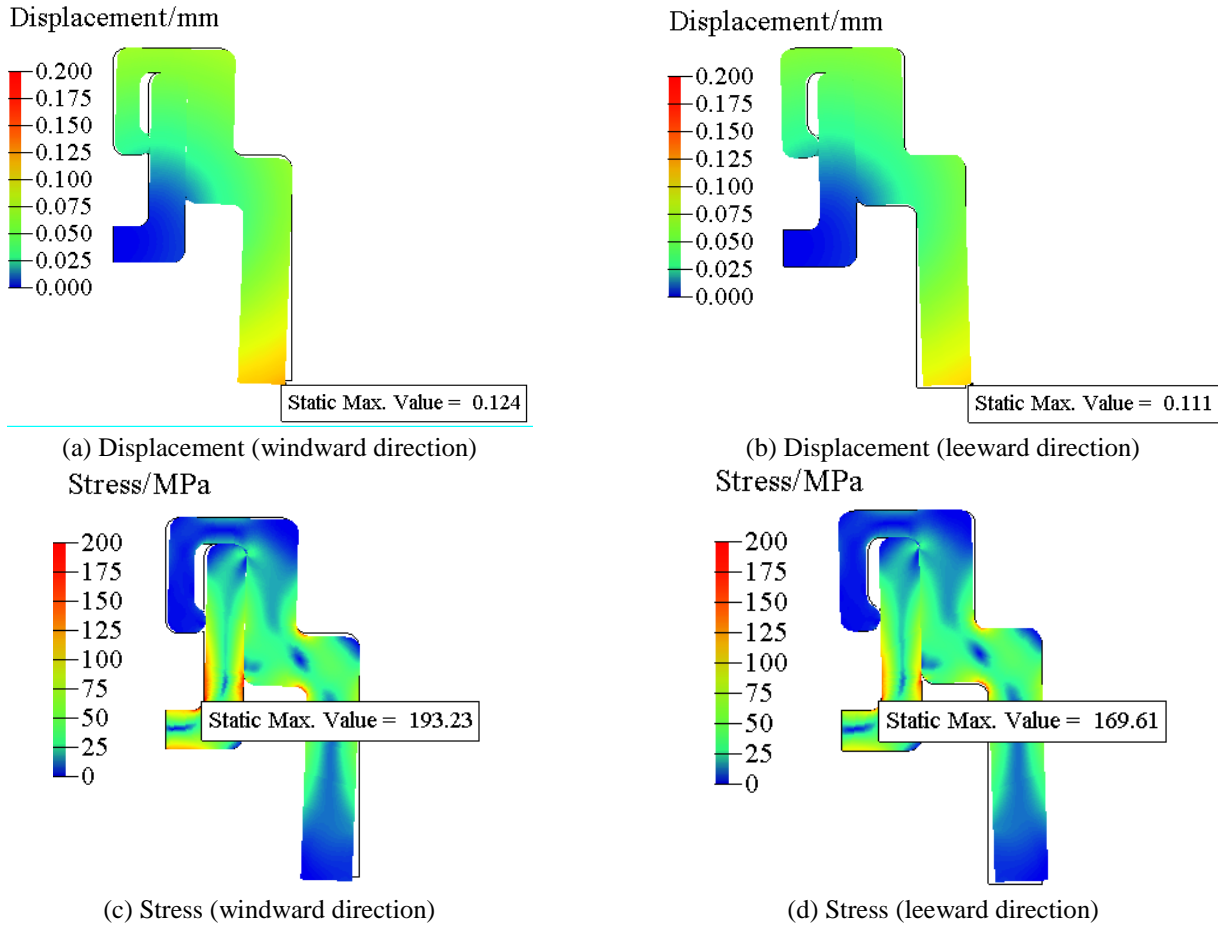


Fig. 6 Structural responses of the conventional design connector

initial gap opening is defined as zero. The normal stiffness of each gap element is calculated by the stiffness of surrounding elements. No bonding stiffness exists when separation occurs.

3.4 Numerical results

The FEA calculation is conducted by OptiStruct. The connector is divided into 3214 quadrilateral elements, 1741 of the hook and 1473 of the catch. The finite mesh of the connector consists of 115 triangular elements and 3099 rectangular elements. The maximum size of the elements is 0.3 mm. The schematic diagram of the meshed finite elements is shown in Fig. 5(b) and Fig. 5(d). Note that the meshes in Fig. 5(b) and Fig. 5(d) are for illustrative purposes and not shown in the real size, finer meshes are employed during the optimization and analysis procedure.

The displacement and stress responses of the conventional design connector are shown in Fig. 6. The maximum displacement occurs at the foot of the hook subjected to the windward load. The maximum displacement is 0.124 mm. The node with maximum displacement is marked out in Fig. 6(a). The maximum stress is 193.23 MPa subject to the windward load, which is within the allowable stress of 210 MPa. The maximum stress occurs at the corner of the catch as Fig. 6(c) shows.

To reduce the stress, one of the commonly applied

methods is to extend the cross-section dimension. However, extension of the geometry dimension will increase material use and self-weight. The material waste of the conventional design is caused by non-optimized material distribution, i.e., the material is not distributed along the load transfer path. To reduce the structural responses and optimize the material distribution, topology optimization is necessary in designing the PV panel connector.

4. Optimized design

Topology optimization preserves only the material on the major stress transferring path. The conventional connector design is optimized by the procedure described in Section 2. The flowchart of the procedure is shown in Fig. 2. The design domain enlarges the conventional design to a more general shape. The topology optimization is to get the optimized topology for the PV panel connector. The post analysis improves the optimized topology to get the practical optimized design.

4.1 Topology optimization

Topology optimization increases the efficiency of material use, hence reduces the material amount. Via topology optimization, the finite elements with larger von

Mises stress, i.e., the elements on the load transferring path, are preserved. The connector is divided into finite elements, and the design variables are the density of each element. The solid isotropic material with penalty (SIMP) method is employed in the topology optimization, which is also known as the density method. According to the SIMP method, the material density of each finite element varies continuously between 0 and 1, representing void or solid element, i.e., ‘remove’ or ‘preserve’ the element. The intermediate values represent fictitious material. The element stiffness is assumed to linearly depend on the density (Spillers and MacBain 2009). Because the elements with intermediate density in the optimized design are not practical, the power law representation of elasticity properties is utilized to force the intermediate density elements to have either 0 or 1 density (Bendsøe 1989). The Young’s modulus of an element is calculated by

$$E(\rho_j) = E_{0,j} \rho_j^p \quad (2)$$

where ρ_j is the density of the j^{th} element. $E_{0,j}$ and $E(\rho_j)$ represent the real and penalized Young’s modulus of the j^{th} element. p is the penalization factor ($p=3.0$ in this study).

The optimized connector design should have minimum structural responses subjected to all the load scenarios, which is a multi-objective optimization problem, therefore, Pareto optimization is employed in this study. The general formulation of the topology optimization is

$$\begin{aligned} \text{Find: } \mathbf{\rho} &= \{\rho_1 \quad \rho_2 \quad \dots \quad \rho_n\}^T \in \mathbb{R}^n \\ \text{Minimize: } C &= \sum w_i C_i = \frac{1}{2} \sum w_i u_i^T f_i \\ \text{Subject to: } &\begin{cases} \rho_{j,\min} < \rho_j < 1, & j = 1, 2, \dots, n \\ \text{Volfrac}_{\min} \leq \text{Volfrac} \leq \text{Volfrac}_{\max} \end{cases} \end{aligned} \quad (3)$$

where ρ_j represents the j^{th} design variable, i.e., the density of the j^{th} element. The objective is to minimize the weighted compliance considering multiple load scenarios. w_i is the weight of the i^{th} load scenario. In this study, two load cases are considered (i.e., windward and leeward load). Because the occurrence probability of both load cases are the same, the weight of both load cases are assigned to 0.5, i.e., equally significant.

C_i stands for the compliance of the i^{th} load case, and is calculated by

$$C_i = \frac{1}{2} u_i^T f_i \quad (4)$$

where f_i and u_i represent the force and the displacement produced by the force along the same degree of freedom of the i^{th} load scenario, respectively.

The density of each element is constraint to be in the parameter space of ρ_{\min} to 1. The lower bound is set to be $\rho_{\min}=0.01$ instead of the theoretically defined zero to ensure the numerical stability. The volume fraction is constraint to ensure the rationality of optimized design. ‘Volfrac’ is the volume fraction of the optimized design, which is defined as

$$\text{Volfrac} = \frac{V_i - V_{\text{non}}}{V_{\text{ini}}} \quad (5)$$

where V_i represents the total volume at current iteration, which refers to the total preserved volume of the connection at the current iteration of the topology optimization, counting all the solid and semi-density elements with corresponding density. V_{non} is the non-design volume, i.e., the total volume of the non-design domain, which remains the same during the topology optimization. In this study, the hook inferior the bolting surface is the non-design domain. V_{ini} stands for the initial design volume, which is the volume of the design domain. The upper/lower limits of the volume fraction are determined according to general optimization experience. The volume fraction is between 30%~60% when the optimization result is stable and reliable (Altair Engineering Inc. 2013), i.e., $\text{Volfrac}_{\min}=0.3$ and $\text{Volfrac}_{\max}=0.6$.

The thickness of the conventional connection is 2~4 mm, as shown in Fig. 4. The average thickness is 3 mm. The width and height dimension of the design domain outline maintain the same with the conventional design. The connecting part of the catch and hook remains the same to guarantee the construction requirements. The design domain is shown in Fig. 7, with loading scenario and boundary condition similar as shown in Fig. 5(a) and Fig. 5(c). The loads are assumed to evenly distribute along the bolting and right border, similar with the conventional design as shown in Fig. 5(b) and Fig. 5(d).

The optimization is conducted by OptiStruct with topology optimization formulation shown in Eq. (3). The design variables are the density of the meshed elements. In the design domain, the catch is meshed with 648 elements, and the hook is meshed with 2519 elements. The total number of the design variables is 3167 (i.e., in Eq. (3), $n = 3167$). The optimization result of the connector is shown in Fig. 8. Fig. 8(a) shows the element density of the optimized topology by diverse colors. From red to blue, the element density reduces from 1.00 to 0.01. For practical design, the

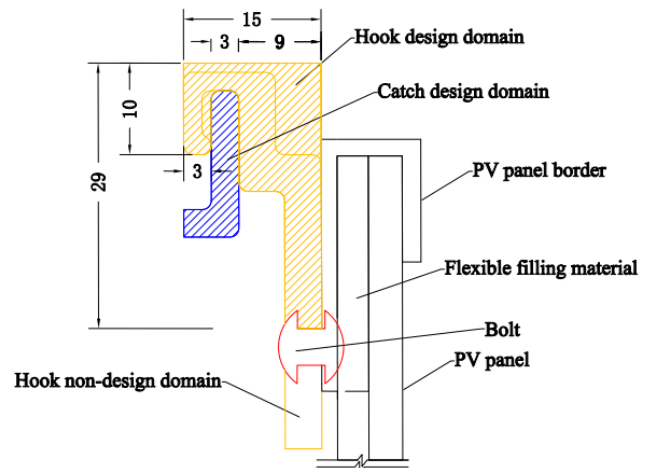
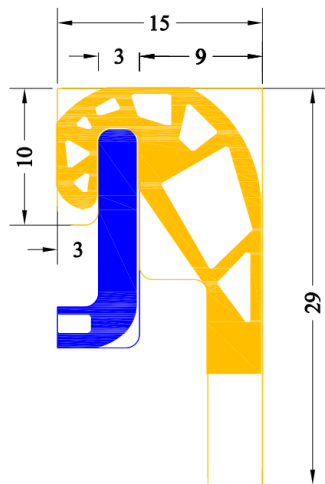
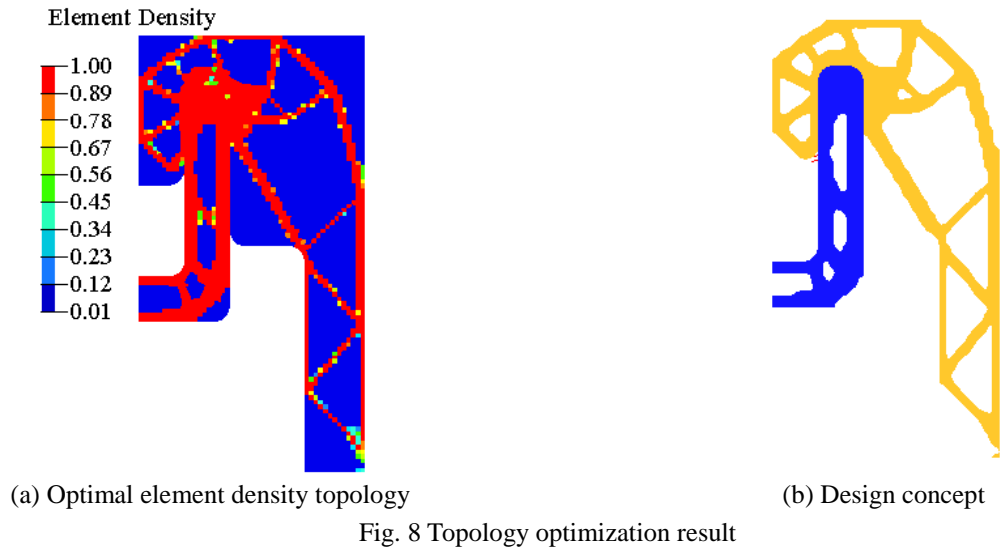


Fig. 7 Design domain of the topology optimization (unit: mm)

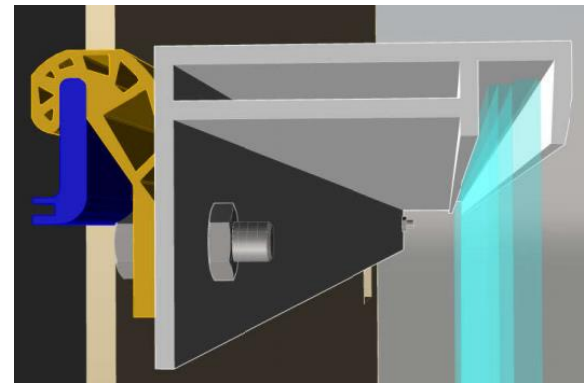


elements with density larger than 0.7 are preserved and assigned to be solid elements, i.e., density is 1.00, as shown in Fig. 8(b).

In Fig. 8, approximately, the volume fraction equals to the total volume of all elements divided by the volume of the red elements. Theoretically, the volume fraction is defined as the sum of the element number (i.e., every element is with the density of 1.00) divided by the sum of each element's density (e.g., elements in red represent density of 1.00, and in blue represents 0.01). The volume fraction of the optimal topology in Fig. 8 is 0.53, which falls within the upper and lower limits, i.e., 0.6 and 0.3, respectively.

4.2 Post analysis

The optimized topology results obtained in Section 4.1 provides the design concept for the optimized PV panel connector. The theoretical optimized result includes semi-density elements, which are not practical for manufactory. Also, the small holes and branches in the optimized topology are uneconomical for massive production.



The post analysis combines the optimized topology concept and the consideration of manufactory. During the post analysis, solid and semi-density elements with density larger than 0.7 are preserved to guarantee safety. The manufactory requires appropriate opening on the work piece. The potential optimized design of the PV panel connector is shown in Fig. 9 according to the topology analysis. The outline of the design is consistent with Fig. 8(b). The irregular curves along the outline are approximated by arcs for manufactory.

Fig. 10 shows the 3D schematic diagram of the optimized design. At the end and the non-design area, the bolts can be fixed to connect the hook and the PV panel as the 3D diagram shows. The four corners of the PV panel are connected with the hooks. The hooks are hung upon the catches, which are fixed with the main structure.

4.3 Numerical verification

The numerical analysis is conducted to verify the displacement and stress responses of the optimized design. The gap elements are applied for the contact of the hook and the catch. The loading scenario and boundary conditions are mentioned in Section 3.3.

The analysis results are shown in Fig. 11. The maximized responses are marked out in each load scenario.

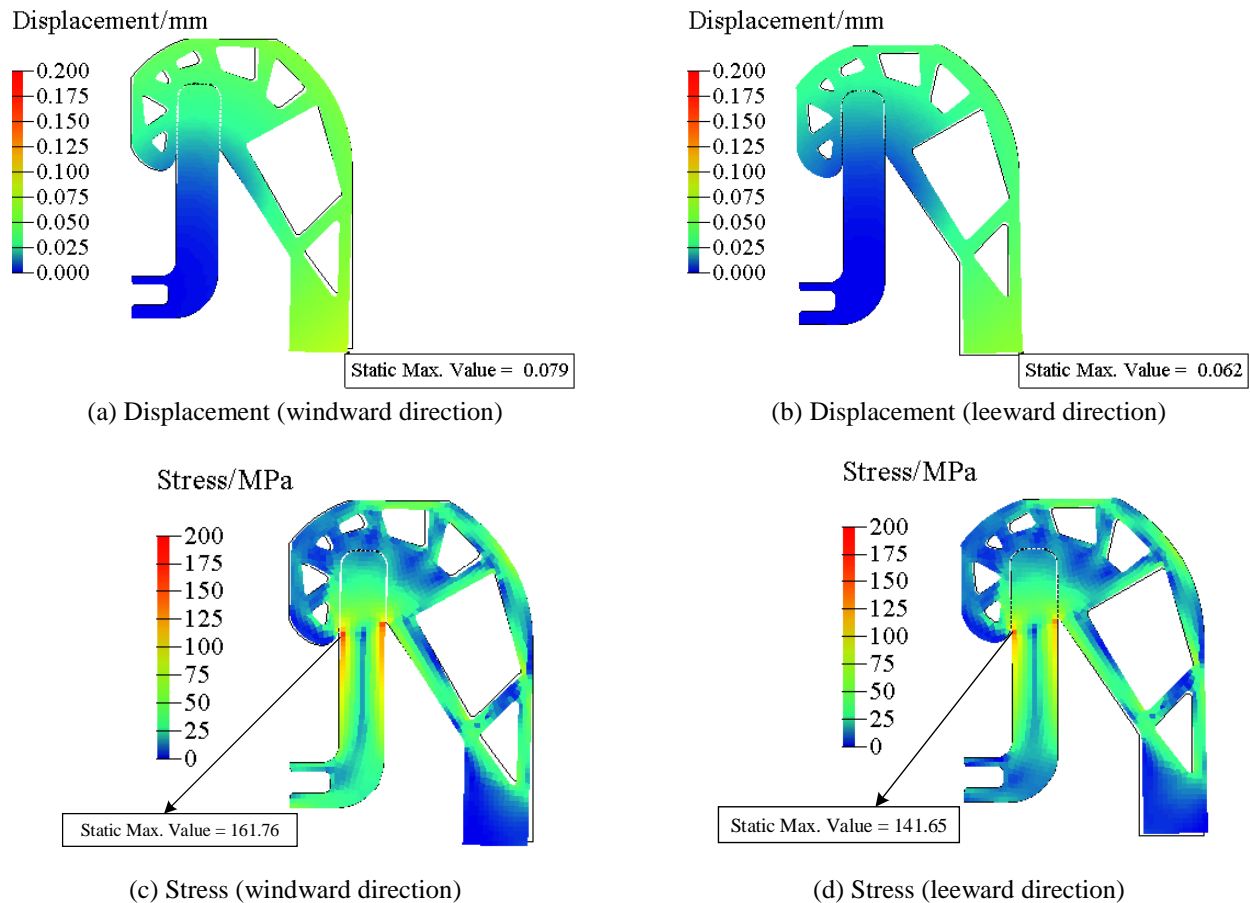


Fig. 11 Structural responses of the conventional design connector

The maximum displacement occurs at the corner of the hook, and the maximum stress is at the edge of the catch. The maximum node displacement is 0.079 mm, and the maximum stress is 161.76 MPa under the load of windward wind load, which is less than the original result (0.124 mm and 193.23 MPa). And the maximum node displacement is 0.062 mm, and the maximum stress is 141.65 MPa under the load of leeward load, which is less than the original result (0.111 mm and 169.61 MPa). The maximum stress is less than the mean yield stress of the steel material (210 MPa), indicating that the hook and catch serve in elastic status when suffering the designed wind loads.

5. Discussion

The PV panel connector without optimization is shown in Fig. 4, and the connection is shown in Fig. 1. In this paper, the cross-section of the conventional design is optimized by the topology optimization procedure. The optimized connector consists of two major parts, hook and catch. The hook is connected with the PV panel via a bolt, and the catch is welded with the main structure. The installation of the PV panel comprises two steps: (i) the hook is bolted with the PV panel frame at the four corners; (ii) the hooks are hung upon the catches. After that, the PV panel can be fixed by limitation components.

In this study, gap elements are employed to connect the two coupled components. When the two components contact together, the gap elements can transit normal force to each other, and when the two parts departure to each other, there will be no interaction. Employing gap elements, the multi-coupled-component topology optimization problem can be solved out.

In order to evaluate the optimization results, the conventional design and the optimized design connector are compared in Table 1. According to the topology results (see Fig. 8), the material distribution of the hook is along the load transferring path and ineffective material is removed from the design domain. The hook area of the optimized design is reduced by 36.8% compared with the conventional design, and 55.2% compared with the design domain. The shape of the optimized catch is similar with the conventional design, except the hollow area at the connecting end. The optimum catch area is decreased by 16.5% compared with the conventional design. Totally, the optimized design reduces about 31.5% volume compared to the conventional design.

The performance of the hook and catch is also compared in Table 1. The maximum node displacement under the windward load reduces 36.3%, and the maximum stress reduces 16.3% concurrently. The maximum node displacement under the leeward load reduces 44.1%, and the maximum stress reduces 16.5%.

Table 1 Comparison of the connectors

Connector	Figure	Hook area (mm ²)	Catch area (mm ²)	Total area (mm ²)	Max Displacement (mm)	Max Stress (MPa)
Conventional design		159.44	56.57	216.01	0.124/0.111	193.23/169.61
Design domain		225.21	56.57	281.78	-	-
Optimized design		100.83	47.24	148.07	0.079/0.062	161.76/141.65

In summary, compared with the conventional design, the optimized connector saves 31.5% material, and furthermore, significantly improves the deformation and stress responses subjected to wind load. Besides, the optimized connector also meets the manufactory requirements.

6. Conclusions

A hook connection of the PV panel with the main structures is optimized by topology optimization in this study. The topology optimization of the connection is an uncertain multi-component coupling problem. The hook and catch are coupled with each other, and the dimension cannot be determined separately. For this reason, gap elements are employed to connect the hook and catch during the optimization procedure. The design concept of the optimized design is based on the topology results and manufactory requirements. The displacement and stress responses of the optimized PV panel connector are compared with the conventional design. The following conclusions can be drawn:

- For the application of topology optimization in the multi-component coupling problem, the gap elements set according to the boundary conditions shows good adaption.
- Engineering application of structural optimization is usually a multi-objective problem considering multiple load scenarios. Pareto optimization is effective in dealing with multi-objective optimization by conducting linear combination of the load scenarios.

- The proposed optimization procedure results in reduction of material volume, along with significant reduction of the maximum displacement and stress simultaneously

In this study, the cross-section of the PV panel connection is designed, which is for the efficacy of the massive production convenience and calculation efficiency. However, with the improvement of the 3D printing techniques, a future study can be pursued to examine the application of the 3D optimization.

Acknowledgments

The authors gratefully acknowledge the financial support provided by HongKong, Macao and Taiwan Science & Technology Cooperation Program of China (Grant No.: 2012DFH70130), National Natural Science Foundation of China (Grant No.: 51578419, 51638012, 11372004), State Key Laboratory of Disaster Reduction in Civil Engineering of Tongji University (Grant No.: SLDRCE14-A-07).

References

- Altair Engineering Inc. (2013), OptiStruct 12.0 user's guide.
- Bendsøe, M.P. (1989), "Optimal shape design as a material distribution problem", *Struct. Optimiz.*, **1**(4), 193-202.
- Erge, T., Hoffmann, V.U. and Kiefer, K. (2001), "The German experience with grid-connected PV-systems", *Solar Energy*, **70**(6), 479-487.
- Fleury, C. (1989), "CONLIN: An efficient dual optimizer based on

- convex approximation concepts”, *Struct. Optimiz.*, **1**(2), 81-89.
- Haftka, R.T. and Gürdal, Z. (2012), *Elements of structural optimization*, Springer Science & Business Media.
- Huang, X. and Xie, Y.M. (2010), “Evolutionary topology optimization of geometrically and materially nonlinear structures under prescribed design load”, *Struct. Eng. Mech.*, **34**(5), 581-595.
- Kaveh, A., Shojaei, I., Gholipour, Y. and Rahami, H. (2013), “Seismic design of steel frames using multi-objective optimization”, *Struct. Eng. Mech.*, **45**(2), 211-232.
- Kutyłowski, R. and Rasiak, B. (2014), “The use of topology optimization in the design of truss and frame bridge girders”, *Struct. Eng. Mech.*, **51**(1), 67-88.
- Lee, D.K., Kim, J.H., Starossek, U. and Shin, S.M. (2012), “Evaluation of structural outrigger belt truss layouts for tall buildings by using topology optimization”, *Struct. Eng. Mech.*, **43**(6), 711-724.
- Lee, E.H. and Park, J. (2011), “Structural design using topology and shape optimization”, *Struct. Eng. Mech.*, **38**(4), 517-527.
- Lund, H. and Mathiesen, B.V. (2009), “Energy system analysis of 100% renewable energy systems-the case of Denmark in years 2030 and 2050”, *Energy*, **34**(5), 524-531.
- Michell, A.G.M. and Melbourne, M.C.E. (1904), “The limits of economy of material in frame-structures”, *Philosoph. Magaz.*, **8**(47), 589-597.
- Ministry of Construction of People’s Republic of China (2001), “Technical code for glass curtain wall engineering (JGJ 102-2003)”, Ministry of Construction of People’s Republic of China.
- Schmit, L.A. and Farshi, B. (1974), “Some approximation concepts for structural synthesis”, *AIAA J.*, **12**(5), 692-699.
- Spillers, W.R. and MacBain, K.M. (2009), *Structural optimization*. Springer Science & Business Media.
- Strahs, G. and Tombari, C. (2006), *Laying the foundation for a solar America: the million solar roofs initiative*. National Renewable Energy Laboratory (NREL), Golden, CO.
- Thomas, H.L., Vanderplaats, G.N. and Shyy, Y.K. (1992), “A study of move limit adjustment strategies in the approximation concepts approach to structural synthesis”, *Proceeding of the Fourth AIAA/USAF/NASA/OAI Symposium on Multidisciplinary Analysis and Optimization*, Cleveland, OH.
- Wright, M.H. (2004), “The interior-point revolution in optimization: history, recent developments, and lasting consequences”, *Bull. Am. Math. Soc.*, **42**(1), 39-56.
- Yang, H. and Fung, Y. (2003), “Building-integrated photovoltaic application-its practice in Hong Kong”, *Proceedings of 3rd World Conference on Photovoltaic Energy Conversion*, 2490-2493.
- Zeng, B. (2016), “Progress on application research of dry-fixing stone curtain wall system”, *Adhesion*, (10), 53-56+52.
- Zhang, H., Dong, J., Duan, Y., Lu, X. and Peng, J. (2014), “Seismic and power generation performance of U-shaped steel connected PV-shear wall under lateral cyclic loading”, *Int. J. Photoenergy*, **2014**, 1-15.
- Zhang, S. and He, Y. (2013), “Analysis on the development and policy of solar PV power in China”, *Renew. Sust. Energ. Rev.*, **21**, 393-401.
- Zhou, M., Pagaldipti, N., Thomas, H. and Shyy, Y. (2004), “An integrated approach to topology, sizing, and shape optimization”, *Struct. Multidisciplin. Optimiz.*, **26**(5), 308-317.